

# Precision electron-gamma spectroscopic measurements in $^{75}\text{As}$

Dwaraka Rani Rao, K. Vijay Sai, M. Sainath, and K. Venkataramaniah<sup>a</sup>

Department of Physics, Sri Sathya Sai Institute of Higher Learning, Prasanthinilayam - 515 134, India

Received: 9 May 2005 / Revised version: 29 August 2005 /  
Published online: 26 October 2005 – © Società Italiana di Fisica / Springer-Verlag 2005  
Communicated by C. Signorini

**Abstract.** The decay of  $^{75}\text{Se}$  to levels of  $^{75}\text{As}$  has been studied using an HPGe detector for gamma-ray and a mini-orange electron spectrometer for conversion electron measurements. We identify 38 transitions in this decay, including 18 gamma rays and 16 conversion electron lines reported for the first time. New results also include  $E2$  multipolarity assignment for the 81 keV transition,  $M1$  assignment to three newly observed transitions and  $M1 + E2$  for the 617 keV transition. A revised  $^{75}\text{As}$  level scheme is constructed using the Ritz combination principle through the computer code GTOL. While confirming the existence of 10 well-established levels, two levels at 587 and 859 keV are newly placed into the decay scheme of  $^{75}\text{Se}$ . The interpretation of the observed levels in terms of various theoretical approaches is briefly discussed. The newly placed 586.8 keV  $1/2^-$  and 859.9 keV  $1/2^+$  levels are studied in the light of the Interacting Boson-Fermion Model.

**PACS.** 23.20.Lv  $\gamma$  transitions and level energies – 23.20.Nx Internal conversion and extranuclear effects – 27.60.+j  $90 \leq A \leq 149$

## 1 Introduction

The level scheme of the nucleus  $^{75}\text{As}$  has been extensively investigated over the past fifty years using a variety of experimental techniques [1]. Detailed information on the level structures upto an excitation energy of 900 keV has been sought through gamma-ray and conversion electron spectroscopy following the beta decay of  $^{75}\text{Ge}$  and the electron capture decay of the long-lived ( $t_{1/2} = 121$  d) source  $^{75}\text{Se}$  [2–27]. Supporting information, albeit with lesser precision, over this region has come from a variety of other techniques [28–30, 2–11], *e.g.* radiative neutron capture, Coulomb excitation [27, 31–35], ( $\alpha, xn\gamma$ ) in-beam experiments, particle transfer reaction studies [36] etc. Several theoretical approaches, *e.g.* the many-particle shell model, Coriolis coupling model, the core excitation model, the Interacting Boson-Fermion Model (IBFM) etc., have been pursued to interpret the observed data. Despite continued investigations, a number of open questions still persist even in the low-energy spectrum. The significant questions which need to be addressed include i) the search for certain levels which are seen in reaction data and are expected to be also populated in the beta decay; ii) careful spectroscopic investigations to examine the evidence for unconfirmed or disputed levels; iii) the particular attempt to identify relatively weaker transitions; iv) an exhaustive and careful study of the conversion electron spectra

to clear the reported uncertainties. These questions are described more specifically in the following paragraphs.

A low-lying  $1/2^-$  state expected from the systematics and also from theoretical considerations is indicated around 585 keV from single-particle transfer reaction studies [36]. But it still remains unobserved in decay or any other studies. A level at 859 keV had been proposed from the particle transfer reaction studies and had not been seen in decay or in any other experiments. Also, the possible spin-parity assignments for the 469 keV and the 617 keV levels tentatively proposed in the earlier studies, were not confirmed in later experiments. One of the main reasons for this situation is the fact that the electron capture decaying source  $^{75}\text{Se}$  is an internationally adopted gamma-ray energy and intensity standard for the calibration of germanium detectors. This factor has caused major attention to be focused mainly on relatively stronger transitions in this decay, whereas confirmation of disputed levels requires focus on weaker transitions.

A close look at the earlier conversion electron measurements [10, 11, 37, 38] also reveals a similar situation. Brundrit and Sen [37] measured the internal conversion coefficient ratios using the sum-coincidence method for the 121, 136, 265 and 280 keV transitions only. Grigoriev and Zolotavin [10] determined the  $K$ -conversion coefficients of the 96, 265, 280, 304 and 400 keV transitions. Edwards and Gallagher [11] using Dumond iron-free ring focusing spectrometer measured the  $K$ -conversion coefficients of the 66, 96, 121, 135, 198, 264, 279, 304 and 400 keV

<sup>a</sup> e-mail: kvenkataramaniah@rediffmail.com

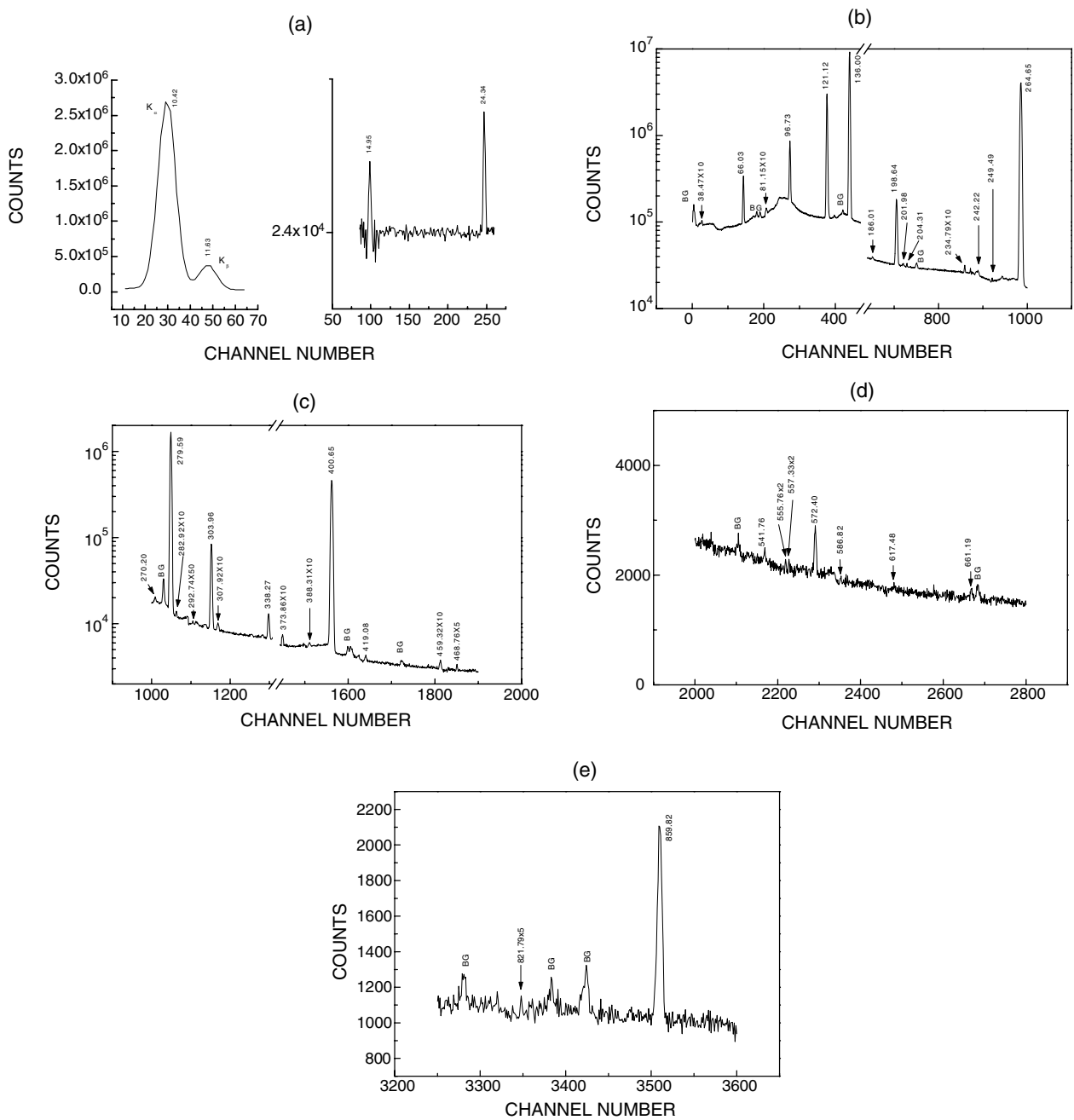


**Fig. 1.** Single  $\gamma$ -ray spectra observed following the EC decay of  $^{75}\text{Se}$  recorded by a Si(Li) detector (*in the low-energy region, panel (a)*) and a 60 cc HPGe detector (*for high energies, panels (b-e)*). The peaks labeled BG arise from other sources.

transitions. Vionova *et al.* [38] measured the conversion coefficients for eight transitions using a spectrometer where there is a simultaneous measurement of the gamma-ray spectrum and of the conversion electron spectrum using cooled Si(Li) and Ge(Li) detectors and assigned multiplicities for eight transitions. No absolute conversion coefficients for  $L$  and  $M$  shells have been reported except for a few  $K/L + M$  ratios in some of the more important transitions. Accordingly, a careful reinvestigation of the complete conversion electron spectrum of the  $^{75}\text{Se}$  decay is called for.

In the present study, we address these questions through precision measurements of gamma-ray energies and relative intensities using an HPGe detector and similar measurements for conversion electrons from the  $^{75}\text{Se}$  decay using a mini-orange electron spectrometer. In sect. 2, we briefly describe the experimental set-up, which is essentially the same as the one employed in our earlier study of the  $^{147}\text{Nd}$  decay [39]. Section 3 includes the results of our measurements and the deduced  $^{75}\text{As}$  level scheme, along with the brief discussion of its interpretation in terms of various theoretical approaches.

Summary and conclusions of our study are given in the final section.

## 2 Experimental procedure

The carrier free sample of the radioactive source  $^{75}\text{Se}$  was obtained from the Board of Radiation and Isotope Technology, Bhabha Atomic Research Centre, Mumbai, India in liquid form as sodium selenosulphate ( $\text{NaSeSO}_4$ ). The  $^{75}\text{Se}$  source was allowed to decay for two half-lives (about 8 months) for the decay of short-lived activities due to contamination (if any). Sources required for acquiring gamma spectra were prepared by drying the source solution on aluminized Mylar foils supported by thin aluminum discs of 1.0 cm diameter. The count rate was kept at around 500 counts/s. Sources required for conversion electron spectroscopy were specially made very thin to avoid backscattering and absorption of the electrons in the source.

Singles gamma spectra were recorded with a 60 cc HPGe detector (FWHM = 665 eV at 5.9 keV ( $^{55}\text{Fe}$ ) and 1.80 keV at 1.33 MeV ( $^{60}\text{Co}$ )) coupled to a 4K PC-based multichannel analyser. Gamma singles spectra were acquired at a source-detector distance of 25 cm. Counting periods lasted an average of  $4.5 \times 10^5$  s per spectrum. The efficiency calibration for the HPGe detector was done using standard radioactive sources. The low-energy 14.95 keV and 24.34 keV spectrum was acquired using a Si(Li) detector (FWHM = 190 eV at 5.9 keV ( $^{55}\text{Fe}$ )). The gamma-ray peaks were analysed using the computer codes FIT [40] and GAMMA VISION [41].

The conversion electron measurements employed a mini-orange spectrometer comprising of i) a windowless Si(Li) detector (surface area = 78 mm<sup>2</sup>, sensitive depth = 5.3 mm, FWHM = 1 keV at 115 keV and 2.3 keV at 624.5 keV), and ii) a mini-orange filter comprising of nine thin wedge-shaped permanent magnets fixed in an orange array in a circular brass frame of 16.2 cm diameter, with a central absorber made of lead to prevent direct exposure of the Si(Li) to photons from the source. A clean vacuum of about  $10^{-6}$  mbar was maintained. The transmission curve was optimized using a  $^{131}\text{Ba}$  source for the best transmission over the electron energies from 40 keV to 800 keV at a source-to-magnet distance of 7.5 cm and a magnet-to-detector distance of 4.5 cm. The optimisation for the low-energy (10–100 keV) region was done by using a  $^{153}\text{Gd}$  source.

Our determination of internal conversion coefficients (ICCs) employs the normalized-peak-to-gamma (NPG) method of using the relative conversion electron and gamma-ray intensities normalized via the conversion coefficient of the intense 264.65 keV transition. The multipolarities of various transitions were derived from the comparison of data with the tables of Hager and Seltzer [42].

In the present work, mixing ratios for gamma transitions are calculated using the experimental value of  $\alpha_K$  and the  $E2$  and  $M1$  conversion coefficients from Hager and Seltzer tabulations [42].

**Table 1.** Comparison of our measured gamma energies with the corresponding values for the transitions adopted as international (IAEA-1998) gamma energy calibration standards. Numbers within the parentheses denote the uncertainties in the last digit(s).

Gamma energies (keV)		
Present Work	IAEA-1998	Longoria-1997
96.732(3)	96.734(1)	96.734(1)
121.118(4)	121.116(1)	121.117(2)
136.000(4)	136.000(1)	136.001(1)
198.640(3)	198.606(1)	198.605(3)
264.654(4)	264.658(1)	264.658(2)
279.580(3)	279.542(1)	279.543(2)
400.653(3)	400.657(1)	400.659(1)

Using the experimentally determined mixing ratios, and the precise values of the lifetimes of the given states, the reduced transition probabilities  $B(E2)$  have been determined using the relation involving the mixing ratio given by

$$B(E2)(e^2b^2) = \frac{0.56563 \times 10^2}{(1 + \alpha)(1 + 1/\delta^2)} E_\gamma^5 T_{1/2}$$

where  $\alpha = \alpha_K + 1.33\alpha_L$ ,  $E_\gamma$  is in keV and  $T_{1/2}$  is in seconds.

## 3 Results and discussion

Now we present the results of our gamma-ray and conversion electron measurements and discuss the placement of the observed transitions in a revised level scheme of  $^{75}\text{As}$ .

### 3.1 Gamma-ray and conversion electron transitions

Typical gamma spectra from the experiment are shown in figs. 1(a-e). In order to conclusively establish our identification of the as-yet unconfirmed weaker transitions and their precise energies, we compare in table 1 the most recent (IAEA-1998) energy calibration standards and another recent compilation [27] with our results. It is seen that almost in all cases the deviations are comparable to the assigned uncertainties; the average deviation for the eight transitions is less than 8 eV. This excellent agreement of our measured gamma energies and the adopted ‘‘benchmark’’ values in the IAEA calibration standard tables and other similar standardization measurements provides us with a firm basis for the identification of new transitions and also for the use of our measured gamma energies to arrive at a revised level scheme for  $^{75}\text{As}$  through the computer code GTOL [43].

A complete listing of the energies and the relative intensities of the 38 gamma transitions, observed in our

**Table 2.** Gamma energies and relative gamma intensities of the transitions observed in the decay of  $^{75}\text{Se}$  are listed in comparison with earlier reports. The earlier reports include Prasad-77 [18], Stewart-96, [45] and NDS-99 [1]. The last column lists the rounded-off level energies and assigned spin-parities of the initial and final levels in each case.

$E_\gamma$ (keV)	$I_\gamma$				$E_i(I_i^\pi) \rightarrow E_f(I_f^\pi)$
	Prasad 1977	Stewart 1996	NDS 1999	Present Work	
14.95(3)	–	–	$\leq 0.002$	0.035(1)	280(5/2 <sup>-</sup> ) $\rightarrow$ 265(3/2 <sup>-</sup> )
24.34(1)	0.065(8)	0.052(5)	0.0459(20)	0.035(1)	304(9/2 <sup>+</sup> ) $\rightarrow$ 280(5/2 <sup>-</sup> )
38.47(8)	–	–	–	0.0038(3)	860(1/2 <sup>+</sup> ) $\rightarrow$ 822(7/2 <sup>-</sup> )
66.03(1)	1.46(20)	1.86(2)	1.888(18)	1.79(1)	265(3/2 <sup>-</sup> ) $\rightarrow$ 199(1/2 <sup>-</sup> )
81.15(9)	0.012(4)	–	0.013(4)	0.017(1)	280(5/2 <sup>-</sup> ) $\rightarrow$ 199(1/2 <sup>-</sup> )
96.73(1)	5.22(20)	5.65(5)	5.807(33)	5.10(4)	401(5/2 <sup>+</sup> ) $\rightarrow$ 304(9/2 <sup>+</sup> )
121.12(2)	27.1(40)	27.60(31)	29.20(56)	27.40(22)	401(5/2 <sup>+</sup> ) $\rightarrow$ 280(5/2 <sup>-</sup> )
136.00(1)	95.46(600)	98.00(100)	98.9(11)	94.05(75)	401(5/2 <sup>+</sup> ) $\rightarrow$ 265(3/2 <sup>-</sup> )
186.01(5)	–	–	–	0.044(1)	587(1/2 <sup>-</sup> ) $\rightarrow$ 401(5/2 <sup>+</sup> )
198.64(1)	2.48(40)	2.56(2)	2.51(7)	2.42(2)	199(1/2 <sup>-</sup> ) $\rightarrow$ 0(3/2 <sup>-</sup> )
201.98(3)	–	0.005(2)	–	0.018(1)	401(5/2 <sup>+</sup> ) $\rightarrow$ 199(1/2 <sup>-</sup> )
204.31(17)	–	0.0042(16)	–	0.018(1)	469(3/2 <sup>-</sup> , 1/2 <sup>-</sup> ) $\rightarrow$ 265(3/2 <sup>-</sup> )
234.79(12)	–	–	–	0.0098(2)	822(7/2 <sup>-</sup> ) $\rightarrow$ 587(1/2 <sup>-</sup> )
242.22(5)	–	–	–	0.023(1)	860(1/2 <sup>+</sup> ) $\rightarrow$ 617(3/2 <sup>-</sup> )
249.49(14)	0.00016(4)	–	–	0.0067(2)	822(7/2 <sup>-</sup> ) $\rightarrow$ 572(5/2 <sup>-</sup> )
264.65(1)	100	100	100	100	265(3/2 <sup>-</sup> ) $\rightarrow$ 0(3/2 <sup>-</sup> )
270.20(4)	–	–	–	0.037(1)	469(3/2 <sup>-</sup> , 1/2 <sup>-</sup> ) $\rightarrow$ 199(1/2 <sup>-</sup> )
279.59(1)	42.6(8)	42.56(31)	42.43(8)	43.07(34)	280(5/2 <sup>-</sup> ) $\rightarrow$ 0(3/2 <sup>-</sup> )
282.92(19)	–	–	–	0.0047(2)	587(1/2 <sup>-</sup> ) $\rightarrow$ 304(9/2 <sup>+</sup> )
292.74(15)	–	–	–	0.00058(1)	572(5/2 <sup>-</sup> ) $\rightarrow$ 280(5/2 <sup>-</sup> )
303.96(1)	2.26(40)	2.24(2)	2.235(8)	2.27(2)	304(9/2 <sup>+</sup> ) $\rightarrow$ 0(3/2 <sup>-</sup> )
307.92(15)	–	0.007(3)	–	0.0039(1)	572(5/2 <sup>-</sup> ) $\rightarrow$ 265(3/2 <sup>-</sup> )
338.27(5)	–	0.0042(7)	–	0.145(1)	617(3/2 <sup>-</sup> ) $\rightarrow$ 279(5/2 <sup>-</sup> )
373.86(6)	–	0.0032(12)	–	0.0044(2)	572(5/2 <sup>-</sup> ) $\rightarrow$ 199(1/2 <sup>-</sup> )
388.31(7)	–	–	–	0.00063(7)	587(1/2 <sup>-</sup> ) $\rightarrow$ 199(1/2 <sup>-</sup> )
400.65(1)	18.8(6)	19.38(2)	19.47(11)	20.13(16)	401(5/2 <sup>+</sup> ) $\rightarrow$ 0(3/2 <sup>-</sup> )
419.08(4)	0.018(4)	0.022(2)	0.0201(5)	0.035(1)	617(3/2 <sup>-</sup> ) $\rightarrow$ 199(1/2 <sup>-</sup> )
459.32(8)	–	–	–	0.0026(2)	860(1/2 <sup>+</sup> ) $\rightarrow$ 401(5/2 <sup>+</sup> )
468.76(10)	0.0006(1)	0.0028(4)	0.00058(13)	0.0036(2)	469(3/2 <sup>-</sup> , 1/2 <sup>-</sup> ) $\rightarrow$ 0(3/2 <sup>-</sup> )
541.76(5)	0.00022(4)	–	0.000022(3)	0.00074(1)	822(7/2 <sup>-</sup> ) $\rightarrow$ 280(5/2 <sup>-</sup> )
555.76(5)	–	–	–	0.0041(2)	860(1/2 <sup>+</sup> ) $\rightarrow$ 304(9/2 <sup>+</sup> )
557.33(18)	–	–	0.0000016	0.0047(2)	822(7/2 <sup>-</sup> ) $\rightarrow$ 265(3/2 <sup>-</sup> )
572.40(3)	0.050(4)	0.063(1)	0.0604(7)	0.062(1)	572(5/2 <sup>-</sup> ) $\rightarrow$ 0(3/2 <sup>-</sup> )
586.82(7)	–	–	–	0.0084(3)	587(1/2 <sup>-</sup> ) $\rightarrow$ 0(3/2 <sup>-</sup> )
617.67(7)	0.0062(8)	0.0082(7)	0.00753(20)	0.0078(2)	617(3/2 <sup>-</sup> ) $\rightarrow$ 0(3/2 <sup>-</sup> )
661.19(2)	–	–	–	0.0057(3)	860(1/2 <sup>+</sup> ) $\rightarrow$ 199(3/2 <sup>-</sup> )
821.79(11)	0.00028(2)	0.0035(6)	0.000233(17)	0.0015(2)	822(7/2 <sup>-</sup> ) $\rightarrow$ 0(3/2 <sup>-</sup> )
859.83(2)	–	–	–	0.117(2)	860(1/2 <sup>+</sup> ) $\rightarrow$ 0(3/2 <sup>-</sup> )

*study* and shown in figs. 1(a-e), is given in table 2. In addition to a comparison of the present intensity values with NDS-99 [1], results from some of the earlier works are also included. In accordance with the usual convention, the gamma intensities in table 2 are quoted relative to the intense 264.65 keV (assumed  $I_\gamma = 100$ ) transition. *18 new transitions* not given in NDS-99 or any other previous report included in table 2, have been observed. A few of these had earlier been tentatively suggested but do not appear in the evaluated data set of NDS-99. The last column in table 2 gives the placement of each transition between the levels of  $^{75}\text{As}$ , as discussed later in this section.

Typical conversion electron spectra from our study are shown in figs. 2(a-e). Conversion electron intensities and internal conversion coefficients, determined by combining the  $I_{\text{CE}}$  (table 3) with  $I_\gamma$  (table 2) are listed in columns 5-7 of table 3 for the *K*-shell lines, along with comparative values from earlier reports. In table 4, the conversion electron intensities and internal conversion coefficients for the *L*-shell, evaluated from our present work, are reported. As mentioned in the preceding section, we employ the NPG method for determining the conversion coefficient, using the 264.65 keV transition as the standard for normalization with its adopted value of  $\alpha_K(264) = 0.00622(2)$ . The

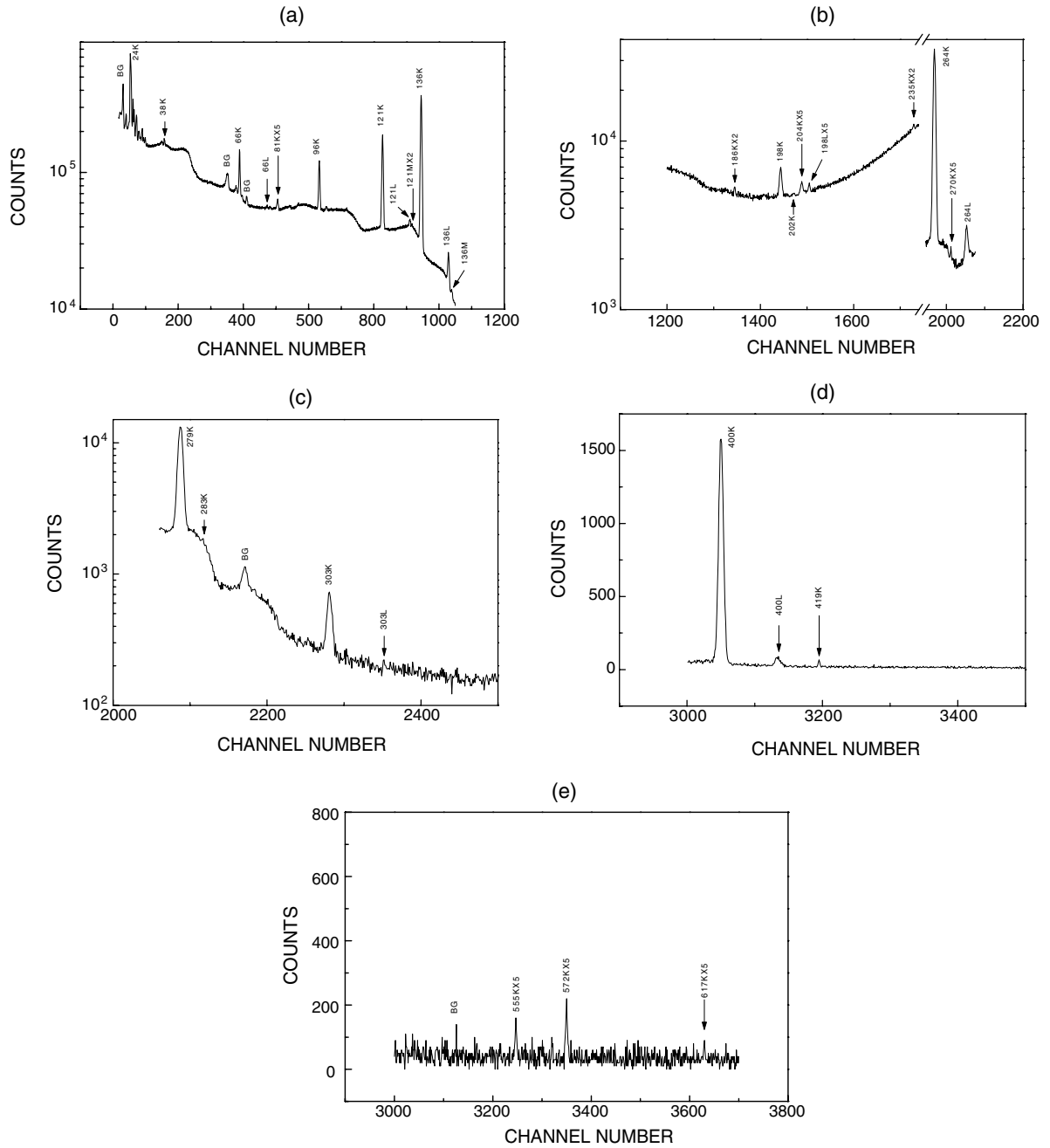


**Fig. 2.** Internal conversion spectra following the EC decay of  $^{75}\text{Se}$  taken with a mini-orange spectrometer.

multipolarity of each transition is then deduced from a comparison of the present  $\alpha_K$  values with the theoretical predictions for possible transitions interpolated from the tables of Hager and Seltzer [42]. In table 5, we compare some of the experimental  $\alpha_K$  values with the corresponding Hager and Seltzer values.

### 3.2 Revised $^{75}\text{As}$ level scheme

Using the precisely determined transition energies and intensities as input data for the application of the Ritz

combination principle, the computer code GTOL [43] has been used to construct the  $^{75}\text{As}$  level scheme. The transition multiplicities, deduced by combining the gamma and conversion electron data, are used to confirm the spin-parity assignments to the respective levels. Well-established undisputed features of this level scheme, as seen in the latest data sheets (NDS-99) [1], are used as crosschecks in our procedure. This process has given the proper placement of the observed transitions and an evaluation of the level energies in the thus constructed level scheme. The results of this exercise are shown in fig. 3 which incorporates all the 38 transitions from our study

**Table 3.**  $K$ -conversion electron data from the decay of  $^{75}\text{Se}$ . The respective columns from the left list the transition energies in  $^{75}\text{As}$ , the relative  $K$ -conversion electron intensities determined by Paradellis [22], Brundrit [37] and in the present experiment, the ICC ( $\alpha_K$ ) from the Paradellis [22], Vionova [38] and the present study and also our deduced multipolarities in comparison with the adopted multipolarities in NDS-99 [1].

$E_\gamma$ (keV)	$I_{CE}$ ( $K$ )			ICC ( $\alpha_K$ )			Multipolarity	
	Paradellis	Brundrit	Present	Paradellis	Vionova	Present	NDS	Present
24.34	1250(150)		1010(1)	178(31)		180(5)	$M2 + E3$	$M2(+E3)$
38.47			205(3)			335(24)		$E3$
66.03	72.3(10)		88.47(20)	0.263(10)		0.308(2)	$M1 + E2$	$M1 + E2$
81.15	4.0(5)		4.04(4)	1.65(35)		1.477(23)	( $E2$ )	$E2$
96.73	724(69)	750(75)	502(1)	0.88(10)	0.776(24)	0.613(1)	$E2$	$E2$
121.12	174(17)	167(20)	169.91(27)	0.0405(17)	0.0381(9)	0.0384(3)	$E1$	$E1$
136.0	399(32)	520(50)	377.94(41)	0.0286(11)	0.0283(12)	0.0250(2)	$E1$	$E1$
186.01			0.664(17)			0.094(3)		$M2$
198.64	7.36(41)	7(1)	6.41(5)	0.0192(12)	0.0169(6)	0.0166(2)	$M1 + E2$	$M1 + E2$
201.98			0.209(9)			0.072(3)		$M2$
204.31			0.068(5)			0.024(2)		$M1 + E2$
234.79			0.356(12)			0.226(9)		$M3$
264.65	100	100	100	0.00622(13)	0.00628(12)	0.00622	$M1 + E2$	$M1 + E2$
270.20			0.0034(4)			0.0056(6)	$M1$	$M1$
279.59	52.5(23)	52(5)	42.93(22)	0.00778(40)	0.00798(23)	0.0062(1)	$M1 + E2$	$M1 + E2$
282.92			0.299(1)			0.40(2)		$M4$
303.96	16.6(5)	17(2)	16.4(8)	0.0472(23)	0.0456(15)	0.045(2)	$E3$	$E3$
400.65	3.71(4)		3.98(4)	0.00114(4)	0.00120(6)	0.00123(2)	$E1$	$E1$
419.08	0.0066(7)		0.012(4)	0.00179(36)		0.00204(58)	( $M1 + E2$ )	$M1 + E2$
555.76			0.0095(32)			0.014(5)		$E4$
572.40	0.0099(9)		0.0103(34)	0.0010(1)		0.0010(3)	$M1 + E2$	$M1 + E2$
617.67	0.0085(9)		0.0011(4)	0.0007(1)		0.00086(33)	( $M1 + E2$ )	$M1 + E2$

**Table 4.**  $L$ - and  $M$ -shell relative conversion electron intensities and the internal conversion coefficient data from the decay of  $^{75}\text{As}$ , as reported in the present work.

Energy (keV)		$I_{CE}$ ( $L$ )	ICC ( $\alpha_L$ )	$I_{CE}$ ( $M$ )	ICC ( $\alpha_M$ )	Multipolarity
66.03	$L$	8.24(6)	0.0287(3)			$M1 + E2$
121.12	$L$	16.96(9)	0.00385(4)			$E1$
	$M$			2.73(4)	0.00062(1)	
136.00	$L$	37.64(13)	0.00249(2)			$E1$
	$M$			5.77(5)	0.000382(4)	
198.64	$L$	0.47(1)	0.00122(4)			$M1 + E2$
264.65	$L$	8.76(6)	0.00054(1)			$M1 + E2$
303.96	$L$	1.724(27)	0.00473(8)			$E3$
400.65	$L$	0.41(1)	0.000126(4)			$E1$

into the revised level scheme, as compared to just 20 gammas placed in the adopted level scheme of NDS-99.

All the eight negative-parity and the two positive-parity levels in the adopted scheme of NDS-99 appear in our level scheme with the excitation energy and the spin-parity assignment agreeing in each case. Two levels with excitation energies 587 and 859.9 keV are newly placed into the decay scheme of  $^{75}\text{Se}$ . Ten out of the eighteen new gammas identified by us pertain to these levels.  $\text{Log}ft$  values calculated using the present data on level energies and intensities of the gamma transitions using a  $\text{Log}ft$

calculator [44], have been incorporated into the new decay scheme.

### 3.2.1 The 617.7 keV level

A level at 618 keV was first reported by Varma and Eswaran [12] and Rao *et al.* [14]. This level also was Coulomb excited by  $\alpha$ -particles and 35–36 MeV oxygen ions. Gamma transitions of energies of 617.8, 419.3, 353.3 and 338.5 keV were observed in the  $^{75}\text{Se}$  electron capture

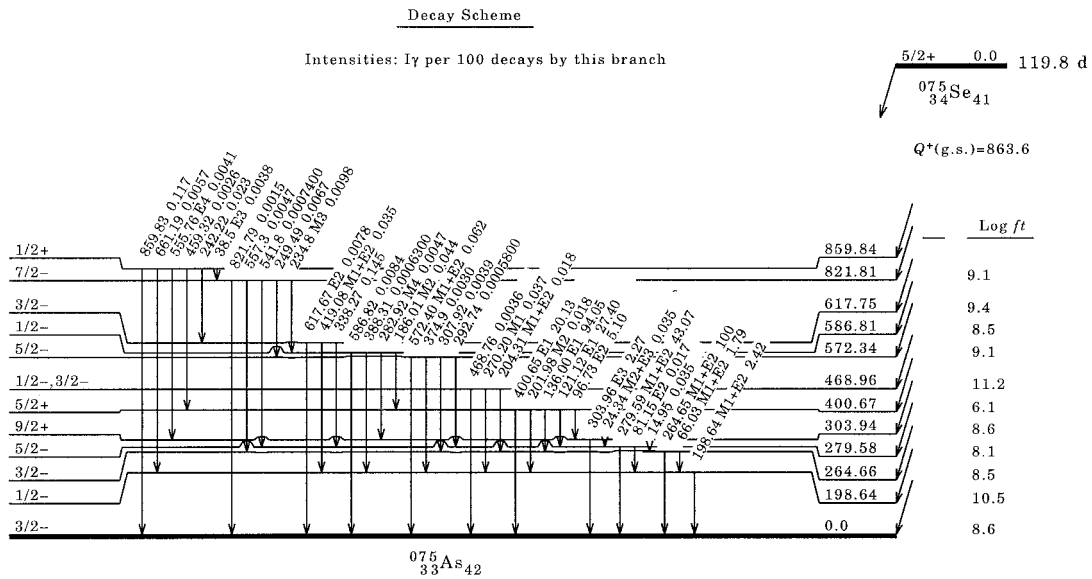


**Fig. 3.** Level scheme of  $^{75}\text{As}$  deduced from gamma and conversion electron spectra measurements following the  $^{75}\text{Se}$   $\beta$ -decay. The labeling on the left is that of the level spin and its parity, while that on the right is the level energy (in keV) deduced from the transition energies listed in table 2 and the energy sum rule at each level.

**Table 5.** Comparison of some of the experimental  $\alpha_K$  values with the corresponding Hager and Seltzer values.

$E_\gamma$ (keV)	ICC ( $\alpha_K$ )	
	Experimental	Hager & Seltzer [42]
38.47	335(24)	295 (E3)
186.01	0.094(3)	0.09577 (M2)
234.79	0.226(9)	0.2141 (M3)
282.92	0.40(2)	0.4395 (M4)
555.76	0.014(5)	0.01182 (E4)

decay as well as in the beta decay of  $^{75}\text{Ge}$ . The 353 keV transition could not be observed in the present work. NDS-99 tentatively assigned  $I^\pi = 1/2^-, 3/2^-$  (based on  $L = 1$  for the ( $^3\text{He}, d$ ) reaction) to this level. As seen in the beta decay, this level has three interconnecting gammas; none of these had a known multipolarity.

The present  $K$ -conversion coefficients for the 419 and 617 keV transitions to the 198 keV  $1/2^-$  level and to the ground  $3/2^-$  state indicate  $M1 + E2$  multipolarity for these two transitions. These multiplicities clearly rule out the possibility of  $I^\pi = 1/2^-$  for the 617 keV level which would require the two transitions to be pure  $M1$  and  $E2$  characters, respectively. Thus, an  $I^\pi = 3/2^-$  is confirmed for this level. Hauser-Feshbach calculations due to McMurray *et al.* [35] support this assignment. The mixing ratio ( $\delta$ ) calculated using the present conversion coefficient for the 419 keV transition (0.159(40)), is in agreement with the IBFM predicted value of 0.18. Also  $\delta$  for the 617 keV transition (0.070(27)), is in very good agreement with the corresponding IBFM value of 0.069.

### 3.2.2 587 keV $1/2^-$ level

Betts *et al.* [36] using the  $^{74}\text{Ge}(^3\text{He}, d)$  reaction observed a weak transition leading to a  $1/2^-$  or  $3/2^-$  state at 587 keV. ( $^3\text{He}, d$ ) experiments had suggested an  $L = 1$  transfer level at around 585.7 keV. Also the IBFM [45] predicted a second  $1/2^-$  state at around 585 keV. This level was not observed in the  $^{75}\text{Se}$  or  $^{75}\text{Ge}$  decays nor was Coulomb excited. Guided by the approximate energy of this level, an intense search was made for locating transitions to the already established levels from this as-yet unobserved level at 587 keV. This search has resulted in identifying five gamma transitions with energies 186.01, 234.79, 282.92, 388.31 and 586.82 keV leading to the following energy loops:

- i) The 822 ( $7/2^-$ ) level decays by a 234.79 keV gamma yielding the daughter at 587.02 keV.
- ii) The decay gamma of 186.01 keV from this new level to 401 keV ( $5/2^+$ ) yields a level energy of 586.68 keV.
- iii) The decay gamma of 282.92 keV to 304 keV ( $9/2^+$ ) yields a level energy of 586.86 keV.
- iv) 388.31 keV gamma connects this level to 198.64 keV  $1/2^-$  resulting in a level energy of 586.95 keV.
- v) The energy of the gamma from this level to the  $3/2^-$  ground state is 586.82 keV.

The use of the computer code GTOL has returned an energy of 586.81 keV for this level. In view of these results the 586.81 keV level is being introduced.

The  $\alpha_K$  of the 186 keV gamma connecting this level to the 401 keV  $5/2^+$  level indicates an  $M2$  character for this transition. This suggests an  $I^\pi = 1/2^-$  for the 587 keV level. The  $K$ -conversion coefficient of the 234.79 keV transition from the 822 keV ( $7/2^-$ ) level leads to the assignment of  $M3$  multipolarity for this transition. This requires

$I^\pi$  for the 587 keV level to be  $1/2^-$ . Finally the evaluated  $\alpha_K = 0.40(2)$  for the 282.92 keV transition to the 304 keV  $9/2^+$  level is very well in agreement with the theoretical  $M4$  value of 0.43, thus establishing an  $M4$  multipolarity for the 282.92 keV transition. These arguments confirm unambiguously the  $I^\pi$  for the 587 keV level as  $1/2^-$ .

### 3.2.3 859.9 keV $1/2^+$ level

Betts *et al.* [36] using the  $^{74}\text{Ge}(^3\text{He}, d)$  reaction observed the  $L = 0$  transfer level at around 859 keV. Schrader *et al.* [46] also observed the  $L = 0$  transfer level at  $862 \pm 5$  keV. Also Coriolis coupling model [47] predicts a positive-parity state around this energy. This level was not observed in the earlier decay studies. An extensive search has resulted in the observation of weak gamma transitions of energies of 38.47, 242.22, 555.76, 661.19 and 859.8 keV leading to the following energy loops:

- i) The decay gamma of 38.47 keV from this new level to 821.81 keV ( $7/2^-$ ) yields a level energy of 859.9 keV.
- ii) The decay gamma of 242.22 to 617.7 keV ( $3/2^-$ ) gives the level energy of 859.92 keV.
- iii) The decay gamma of 555.76 to 304 keV ( $9/2^+$ ) yields the level energy of 859.76 keV.
- iv) The decay gamma of 859.8 to the  $3/2^-$  ground state gives the level energy of 859.8 keV.
- v) The decay gamma of 459.32 to the 400.67 keV  $5/2^+$  state gives the level energy of 859.97 keV.

Also the use of the computer code GTOL to fit the new gammas has resulted in the energy of this new level as 859.9 keV.

In addition to these four new gamma transitions, the  $K$ -conversion lines corresponding to the 38.47 and 555.76 keV gammas have also been observed. The  $\alpha_K$  of the 38.47 keV transition from this level to the 822 keV  $7/2^-$  level indicates an  $E3$  multipolarity for this transition. This suggests an  $I^\pi$  of  $1/2^+$  for the 859.9 keV level. Also the  $K$ -conversion coefficient of the 555 keV transition to the 304 keV,  $9/2^+$  level leads to an assignment of  $E4$  multipolarity for the 555 keV transition. This establishes an  $I^\pi$  of  $1/2^+$  for this 859.9 keV level, which was not observed as Coulomb excited or seen in photo-excited decay. The  $1/2^+$  present assignment to this level agrees with that from the transfer reaction. This level can be identified with the  $J = 1/2$  level observed at 868 keV by Betts *et al.* [36]. A level at 860.8 keV was reported also by Schrader *et al.* [46].

### 3.3 Model description

The Interacting Boson Model (IBM) [48] and its extension to the odd- $A$  nuclei, the Interacting Boson-Fermion Model (IBFM) [49], have been applied by Stewart and Radhi [45] to account for the low-energy level structure and electromagnetic properties of the  $Z = 33$ ,  $^{75}\text{As}$  nucleus.

In the IBFM formalism, the  $^{75}_{33}\text{As}$  nucleus is seen as a single fermion (proton) coupled to the even-even  $^{74}_{32}\text{Ge}$

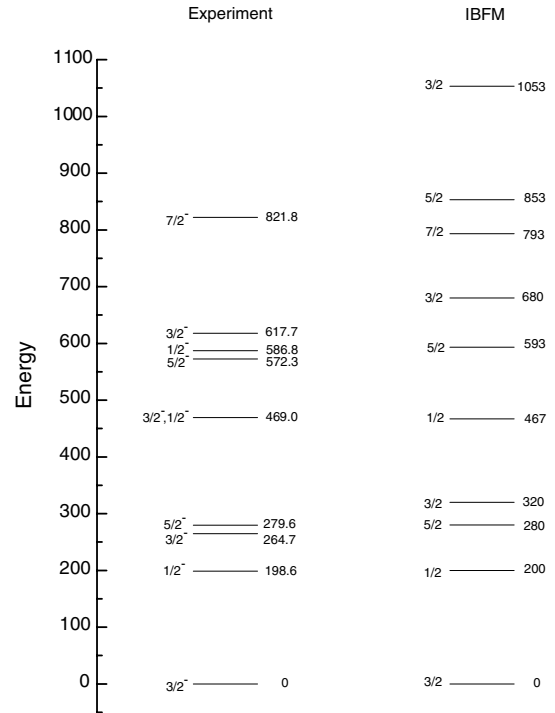


**Fig. 4.** Comparison of the experimental negative-parity levels of  $^{75}\text{As}$  with those predicted by the IBFM model.

core described by the IBM model. Duval *et al.* [50] used the IBM-2 model, the version of the IBM which takes into account proton and neutron bosons separately, as configuration mixing to describe even-even nuclei in the germanium region.

Stewart and Radhi have carried out an analysis for the odd-mass nucleus  $^{75}\text{As}$  based on the IBFM. The nucleus is described by coupling a single fermion (proton) to the even-even core of  $^{74}\text{Ge}$ . The boson core parameters have been obtained from an IBM-1 analysis. In the IBFM calculations, the odd proton is allowed to occupy the  $2p_{3/2}$ ,  $1f_{5/2}$ ,  $2p_{1/2}$  single-particle orbits. In running the ODDA program, the strategy of varying only one of the parameters  $A_o$ ,  $\Gamma_o$  and  $\Delta_o$  in the boson-fermion interaction term ( $V_{BF}$ ), and keeping the other two unchanged, was used by Stewart and Radhi.

The inclusion of multilevel possibilities into the IBFM has been analysed by Scholten [51] who developed a formalism based on the BCS equations [52]. The single-particle energies were calculated using the relations given by [53].

The results of the IBFM multilevel calculations of Stewart and Radhi for  $^{75}\text{As}$  are compared with the present experimental energy levels in fig. 4.

There is a good agreement with the calculated levels within the experimental limits. The reduced transition probabilities  $B(E2)$  and the multipole mixing ratios ( $\delta$ ) for the transitions in  $^{75}\text{As}$  were also calculated using the IBFM model. These are compared with the present experimental data in table 6. It can be seen that there is a good agreement for the mixing ratios for most of the transitions.



**Table 6.** Comparison of mixing ratios and  $B(E2)$  values from the present study with those of IBFM calculations in  $^{75}\text{As}$ .

Energy (keV)	Transition $J_i \rightarrow J_f$	Mixing Ratio ( $\delta$ )		$B(E2)$ ( $e^2b^2$ )	
		Present	IBFM	Present	IBFM
198.64	$1/2^- \rightarrow 3/2^-$	0.308(15)	-0.32	-	0.033
264.65	$3/2^- \rightarrow 3/2^-$	0.058(5)	-0.05	0.0037(4)	0.0020
279.59	$5/2^- \rightarrow 3/2^-$	0.264(30)	+0.30	0.024(3)	0.020
419.08	$3/2^- \rightarrow 1/2^-$	0.159(40)	+0.18	0.02(1)	-
572.40	$5/2^- \rightarrow 3/2^-$	0.40(12)	+0.43	0.049(15)	0.0682
617.67	$3/2^- \rightarrow 3/2^-$	0.070(27)	-0.069	-	0.0010

Thus, it may be concluded that the IBFM provides a successful description for the energy level properties of the transitional nucleus  $^{75}\text{As}$ .

## 4 Summary and conclusions

Precision measurements of the gamma and internal conversion electron spectra following the  $^{75}\text{Se}$  decay have been undertaken. The precision of the data is established by comparing the present results with the IAEA adopted international calibration standards and other benchmark measurements. A revised level scheme for  $^{75}\text{As}$  is constructed, based on summed energy for various loops, incorporating 38 gamma transitions, in which 18 transitions observed in the present work are not listed in the adopted data set of the latest (1999) Nuclear Data Sheets. The revised level scheme introduces two levels at 587 keV and 859.9 keV, with 10 (out of 18) new transitions connecting these levels with the earlier established levels. 31 conversion lines are being included, 16 of them for the first time. Multipolarities have been assigned for 5 transitions which had no assignments in earlier studies. Based on the present conversion coefficient data, the spin-parity of the 617 keV level has been confirmed as  $3/2^-$ .

The 587 keV level corresponding to the  $L = 1$  level reported in the ( $^3\text{He}, d$ ) reaction studies, is assigned  $I^\pi = 1/2^-$ . This level has been found to be the one predicted by the IBFM model but not seen earlier in the decay studies. The level at 859.9 keV has been assigned an  $I^\pi = 1/2^+$ . Precise mixing ratios and  $B(E2)$  values have been calculated and compared with the IBFM model predictions. It has been observed from the comparison of the experimental data on level energies and electromagnetic moments, that the nuclear structure of the transitional nucleus  $^{75}\text{As}$  could be well understood in the framework of IBFM.

The authors acknowledge the financial support provided by the Department of Atomic Energy, Government of India through DAE-BRNS research project.

## References

1. Ameenah R. Fahan, Balraj Singh, Nucl. Data Sheets **86**, 785 (1999).
2. J.M. Cork, W.C. Rutledge, C.R. Branyan, A.E. Stoddard, J.M. Le Blanc, Phys. Rev. **79**, 889 (1950).
3. E.N. Jensen, L.J. Leslett, D.S. Martin, F.G. Hughes, W.W. Pratt, Phys. Rev. **90**, 557 (1953).
4. A.W. Schardt, J.P. Welker, Phys. Rev. **99**, 810 (1955).
5. W.H. Kelly, M.L. Wiedenbeck, Phys. Rev. **102**, 1130 (1956).
6. A.W. Schardt, J.P. Welker, Phys. Rev. **108**, 398 (1957).
7. H.J. van den Bold, H.C. van den Giejn, P.M. Endt, Physica **24**, 23 (1958).
8. F.R. Metzger, W.B. Todd, Nucl. Phys. **10**, 220 (1959).
9. G. Backstrom, M.D. Cross, Ark. Fys. **16**, 567 (1959).
10. E.D. Grigoriev, A.V. Zolotavin, Nucl. Phys. **14**, 443 (1960).
11. W.F. Edwards, C.J. Gallagher, Nucl. Phys. **26**, 649 (1961).
12. J. Varma, M.A. Eswaran, Phys. Rev. **125**, 656 (1962).
13. S.M. Naqvi, A.J. Dilay, Nucl. Phys. **77**, 665 (1966).
14. P.V. Rao, D.K. McDaniel, B. Crassmann, Nucl. Phys. **81**, 296 (1966).
15. P. Jahn, W. Todt, O. Draguon, Z. Phys. **210**, 245 (1968).
16. H. Vignau, A. Mocora, R. Othaz, J. Voss, B. Wolbeck, G. Dammertz, K.G. Plingen, Nucl. Phys. **115**, 421 (1968).
17. T.S. Nagpal, Nucl. Phys. **121**, 176 (1968).
18. Rajendra Prasad, Can. J. Phys. **55**, 2036 (1977).
19. D.E. Raeside, M.A. Ludington, J.J. Reidy, M.L. Wiedenbeck, Nucl. Phys. **130**, 677 (1969).
20. T. Paradellis, S. Hontzeas, Nucl. Phys. **131**, 378 (1969).
21. A.J. Becker, R.M. Steffen, Phys. Rev. **180**, 1043 (1969).
22. T.H. Paradellis, S. Hontzeas, J. Phys. **48**, 2254 (1970).
23. W.W. Pratt, Nucl. Phys. **170**, 223 (1971).
24. C.H. Johnson, Phys. Rev. **136**, 1719 (1964).
25. R.N. Thomas, R.V. Thomas, J. Phys. A **6**, 1037 (1973).
26. J.L. Campbell, J. Phys. A **7**, 1451 (1974).
27. L.C. Longoria, J.N. Benitz, Appl. Radiat. Isotopes **48**, 1069 (1997).
28. B.R. Mottelson, S.G. Nilsson, Mat.-Fys. Medd. K. Dan. Vidensk. Selsk. **1**, No. 8 (1959).
29. M. Ter-Pegossian, J.E. Robinson, C.S. Cook, Phys. Rev. **75**, 995 (1949).
30. R.L. Robinson, F.K. McGowan, P.H. Stinson, W.T. Milner, Nucl. Phys. A **104**, 401 (1967).
31. G.M. Temmer, N.P. Heidenberg, Phys. Rev. **104**, 967 (1950).
32. H. Kamitsubo, J. Phys. Soc. Japan **17**, 253 (1961).
33. R.C. Ritter, P.H. Stelson, F.K. McGowan, R.L. Robinson, Phys. Rev. **128**, 2320 (1962).
34. N. Imanishi, M. Sakisaka, F. Fukuzava, Nucl. Phys. **125**, 626 (1969).
35. W.R. McMurray, P.J. Celliers, R. Saayman, Nucl. Phys. A **225**, 37 (1974).
36. R.R. Betts, S. Mordechai, D.J. Pullen, B. Rosner, W. Scholz, Nucl. Phys. A **230**, 235 (1974).
37. D.R. Brundrit, S.K. Sen, Nucl. Phys. **68**, 425 (1965).
38. N.A. Vionova, A.I. Egerov, Y.V. Kalinchev, A.G. Sergeev, Bull. Acad. Sci. USSR, Phys. Ser. **35**, 794 (1972).
39. M. Sainath, K. Venkataramaniah, P.C. Sood, Phys. Rev. C **56**, 2468 (1997).
40. V. Petkov, Bakaltchev, J. Appl. Crystallogr. **23**, 138 (1990).

41. GAMMA VISION-32, Version 5.10, EG&G, ORTEC (1998).
42. R.S. Hager, E.C. Seltzer, Nucl. Data A **4**, 1 (1968).
43. GTOL Program Package, ENSDAT (Version 3.92) NNDC Brookhaven (1994).
44. Log *ft* Program, Log *FT* 2.1; <http://ie.lbl.gov/programs/logft/logft.html>.
45. M. Stewart, F.S. Radhi, Z. Phys. A **354**, 261 (1996).
46. M. Schrader, H. Reiss, G. Rosner, H.V. Klapdor, Nucl. Phys. A **263**, 193 (1976).
47. W. Scholz, F.B. Malik, Phys. Rev. **176**, 1355 (1968).
48. A. Arima, F. Iachello, Phys. Rev. Lett. **35**, 1069 (1975).
49. F. Iachello, O. Scholten, Phys. Rev. Lett. **43**, 679 (1979).
50. P.D. Duval, D. Goutte, M. Vergnes, Phys. Lett. B **124**, 297 (1983).
51. O. Scholten, PhD Thesis, University of Groningen, 1980.
52. J. Bardeen, L.N. Cooper, J.R. Scribefer, Phys. Rev. **108**, 1175 (1957).
53. B.S. Reehal, R.A. Sorensen, Phys. Rev. C **2**, 819 (1970).